Electrical and Dielectric Properties of Copper Ion Conducting Solid Polymer Electrolytes Based on Chitosan: CBH Model for Ion Transport Mechanism

Shujahadeen B. Aziz [1,2,*], Omed Gh. Abdullah [1,2], Salah R. Saeed [3] and Hameed M. Ahmed [1]

[1] Advanced Polymeric Materials Research Lab., Department of Physics, College of Science, University of Sulaimani, Qlyasan Street, Sulaimani, 46001, Kurdistan Regional Government, Iraq
[2] Komar Research Center (KRC), Komar University of Science and Technology, Sulaimani, 46001, Kurdistan Regional Government, Iraq
[3] Charmo Research Center, Charmo University, Peshawa Street, Chamchamal, Sulaimani, Kurdistan Regional Government, Iraq
[*]E-mail: shujaadeen78@yahoo.com, rshujahadeenaziz@gmail.com

Copper ion-conducting polymer electrolytes based on chitosan (CS) were prepared using solution-cast technique. The CS host polymer was complexed with different weight percent copper iodide (CuI) salt. Effect of frequency, temperature and copper ion concentration on the electrical and dielectric properties has been studied. The high value of dielectric constant at low frequency is an evidence for the presence of space charge polarization. The AC conductivity at higher frequency region obeys a Jonschers power law. Three regions were distinguished in the ac conductivity spectra of the solid polymer electrolyte films. The frequency exponent (*S*) was estimated for the high-frequency regions. Analysis of frequency exponent (*S*) at various temperatures suggested the correlated barrier hopping (CBH) model for ion transport mechanism at high temperatures. The results of the present work, reveals that to get deep insight about the conduction mechanism the frequency exponent (*S*) at different temperature must be studied. The estimated value of dc conductivity obtained from the plateau region of ac conductivity spectra seem to be close to those calculated from the bulk resistance. The electrical modulus analysis shows the non-Debye type conductivity relaxation.

1. INTRODUCTION

The environmentally friendly solid polymer electrolytes based on natural polymers have been receiving great attention recently due to their potential applications in electrochemical devices such as

electrochromic devices, high energy density batteries, sensors and fuel cells [1,2]. The light-weight, flexibility, low cost, abundant, nontoxic and easy throwing away are advantages of natural polymer electrolytes [3]. Various polymer electrolytes based on natural polymers such as Cellulose [4], Methylcellulose [5], Starch [6], Agarose [7], and Chitosan [8] have been developed and characterized previously. Improving the ionic conductivity at ambient temperature is the only requirement for these materials to be used in electrochemical applications [9]. Various polymer electrolytes have been studied previously to achieve the desired polymeric electrolyte materials with improved electrochemical performance [10,11], but so far, the electrical conductivity of solid polymer electrolyte of more than 10^{-3} S/cm has not been realized. This may be related to lake understanding of the conduction mechanism in polymer electrolyte [12, 13]. The electrical conductivity of solid polymer electrolyte mainly depends on the density of charge carriers and carrier mobility. It is well reported that ionic mobility is closely coupled to the motion of the polymer chains above the glass transition temperature (T_g) [14]. A numeral of experimental and theoretical studies have been carried out on different polymer electrolyte systems to understand the ion transport process and some models have been proposed [15, 16]. Preparation of new solid polymer electrolytes requires an electrical characterization in order to understand the cation transport in host polymer [17]. Study the dielectric properties of polymer electrolytes are useful for obtaining particular information regarding the ion-molecular interaction and the ability of a host polymer to dissolve salts [18, 19]. The frequency dependent electrical conductivity is significant to get considerable information on ion dynamics. The electrical conductivity of solid polymer electrolyte depends on factors like concentration of the charge carriers and the rate at which they are mobile from one available site to another. Both the ionic conductivity and dielectric properties depend on the charge carriers motion and polarization of dipoles of the host polymer. The presence of complete information on conductivity and dielectric properties are essential to specify the mechanism of ion conduction in solid polymer electrolytes [13]. In this study the AC conductivity, dielectric constant, dielectric loss, and electrical modulus at various temperatures have been investigated to identify the mechanism of copper ionic transport in chitosan:CuI based solid electrolyte films.

2. EXPERIMENTAL

2.1 Material Preparation

Free-standing polymer electrolyte films were prepared by conventional solution casting technique with Chitosan (CS) from crab-shells, (average molecular weight 1.1×10^5 g/mol) as the polymer host matrix and copper iodide (CuI) provided by Sigma-Aldrich (97% purity, molecular weight 190.45 g/mol) as the salt for complexation. The CuI salt was dried at 140 °C for 6 h to remove surface adsorbed moisture prior to sample preparation. One gram of CS powder was dissolved in 80 mL of 1% acetic acid, and the solution was stirred for 24h at ambient temperature, until completely dissolved and clear viscose solutions were obtained. Subsequently, different amounts of CuI (4, 8, 12, and 16 wt.%) were dissolved in 10 mL acetonitrile (Merck) and added separately to the CS solution.

The mixtures were stirred for 2 h to facilitate homogeneous mixing and complexation. The polymer electrolyte samples were coded as CS1, CS2, CS3, and CS4 for CS incorporated with 4, 8, 12, and 16 wt.% of CuI, respectively. After casting the final polymer-salt complex solutions in different Petri dishes, the solvent was allowed to evaporate slowly at ambient temperature for two weeks for films to form. Finally, the dried freestanding polymer electrolyte films were stored in desiccators for further drying with blue silica gels.

2.2 Materials Characterization

Conductivity and dielectric measurements on the prepared solid polymer electrolyte films were carried out in the frequency range of 50 Hz to 1 MHz using a computer-interfaced impedance analyzer (HIOKI LCR, Model 3532, Japan). The samples were sandwiched between two stainless steel blocking electrodes of the conductivity cell.

3. RESULTS AND DISCUSSION

3.1 Complex Impedance Spectroscopy Analysis

The studies of complex impedance plots are crucial to investigate the electrical conductivity and electrochemical performance of batteries and super-capacitors. The complex impedance plots of the CS:CuI solid polymer electrolyte samples at room temperature (T=303 K) are shown in Fig.1. The electrical impedance plots show two obvious regions at room temperatures. The high-frequency arc and low-frequency spike observed in the impedance plots are ascribed to the bulk conduction process and accumulation of free charges at the electrolyte-electrode interface (blocking electrode) respectively [20,21]. In fact, the low-frequency region of the complex impedance plot must show a straight line parallel to the imaginary axis, but the double layer phenomena causes the inclination [22]. The incomplete semicircular arc of Argand plots with a diameter below the real impedance axis indicates that charge carriers have different relaxation times [23,24]. The intercept of the high-frequency semicircular arc with the real axis of the complex impedance plots represents the electrical bulk resistance (R_b) of the sample. It is obvious from Fig. 1, that R_b value initially decreases with increasing CuI content and reaches to a minimum ($R_b = 740 \ \Omega$) at 8 wt.% CuI content. It is clear that further addition of CuI increased the R_b value. The lowest value of R_b for CS2 indicates that this sample has maximum ionic conductivity. The increase in R_b value for the CS3 and CS4 samples can be ascribed to ion association which usually occurs at high salt concentration, which in turn decreases the conductivity. The change in ionic conductivity σ of polymer electrolyte was affected by carrier density (n) as well as the mobility of charge carriers (μ) [25].
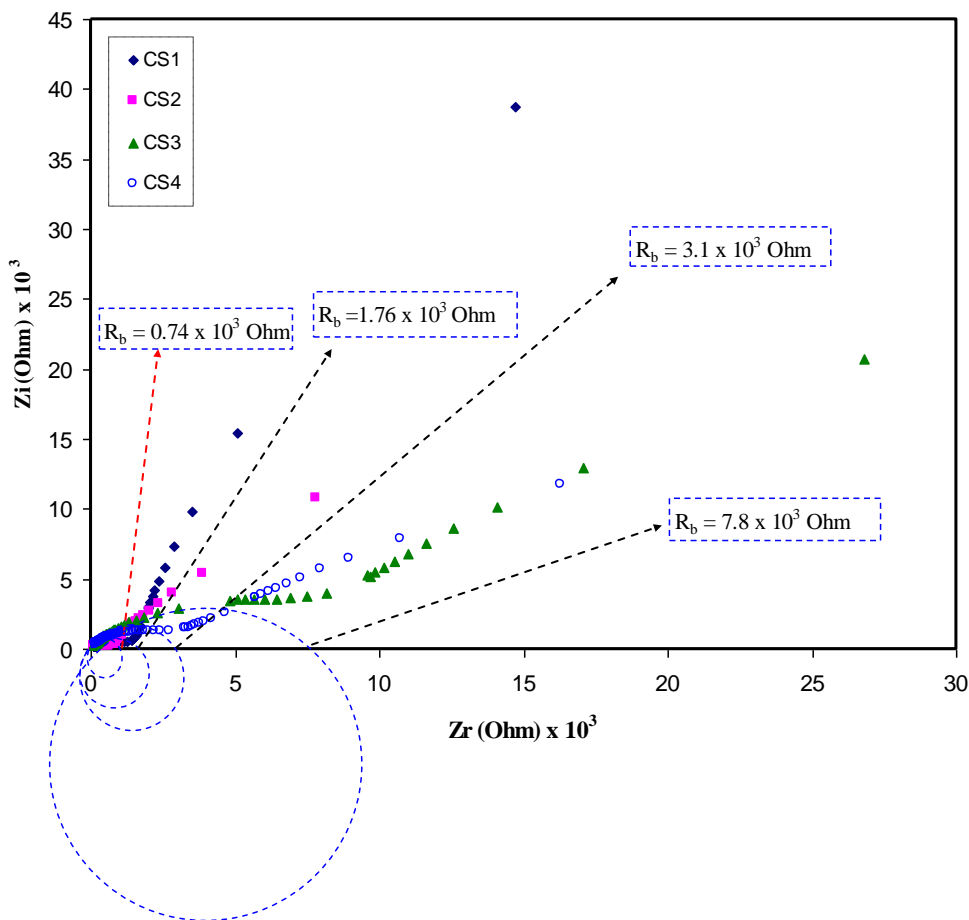
Figure 1. Complex impedance plots for all chitosan solid electrolytes at room temperature. The CS2 sample exhibits the lowest bulk resistance (R_b).

The general expression for the ionic conductivity of a solid polymer electrolyte is given as $\sigma = \sum q_i n_i \mu_i$, where q_i is the ionic charge [26]. Thus the ionic conductivity can be enhanced by either increasing the salt concentration or mobility of charge carriers. It can be noticed that at the intermediate frequency the formation of second semicircle can appear. This can be ascribed to the formation of copper nanoparticles through the host CS polymer [27]. In impedance plots, it is possible to detect the presence of metallic nanoparticles [21, 24]. In our previous works, we observed the reduction of transition metals salts in CS host polymer [2, 20, 21, 24, 27]. Thus the curvature of data points at low and intermediate frequencies is related to the reduction of some of the copper ions to copper metallic nanoparticles.

3.2 Dielectric Analysis

The studies of the real and imaginary parts of the complex dielectric constant are of particular significance for ion conducting polymer electrolytes. Dielectric constant (ε_r), is a measure of material to stored electric charge, whereas dielectric loss (ε_i), is a measure of dissipation energy in the

materials. The real and imaginary parts of the complex dielectric constant can be calculated from the following relations [28,29]:

$$\varepsilon_r(\omega) = \frac{Z_i}{\omega C_o\left(Z_r^{\,2} + Z_i^{\,2}\right)} \qquad (1)$$

$$\varepsilon_i(\omega) = \frac{Z_r}{\omega C_o\left(Z_r^{\,2} + Z_i^{\,2}\right)} \qquad (2)$$

Here $C_o = \varepsilon_o A/l$ is the vacuum capacitance, where ε_o is the free space dielectric permittivity, l is the thickness, and A is the cross-section area of the capacitor. The angular frequency ω is equal to $\omega = 2\pi f$, where f is the frequency of applied ac field.

Figures 2 and 3 show the variation of dielectric constant (ε_r) and dielectric loss (ε_i) versus frequency at room temperature for all the samples. It is evident that the dielectric loss for low salt concentration sample (CS1) exhibits two distinct dispersive regions, characterized by a change in slope. At low frequency, the dielectric loss increases gradually and then decreases progressively in its magnitude at the higher frequency region. The asymmetric-broad dielectric loss peak for CS1 sample suggests a deviation from classical exponential Debye behaviour [30]. As the salt concentration increases, the dielectric parameters show one dispersion region and tend to decrease with increasing frequency.
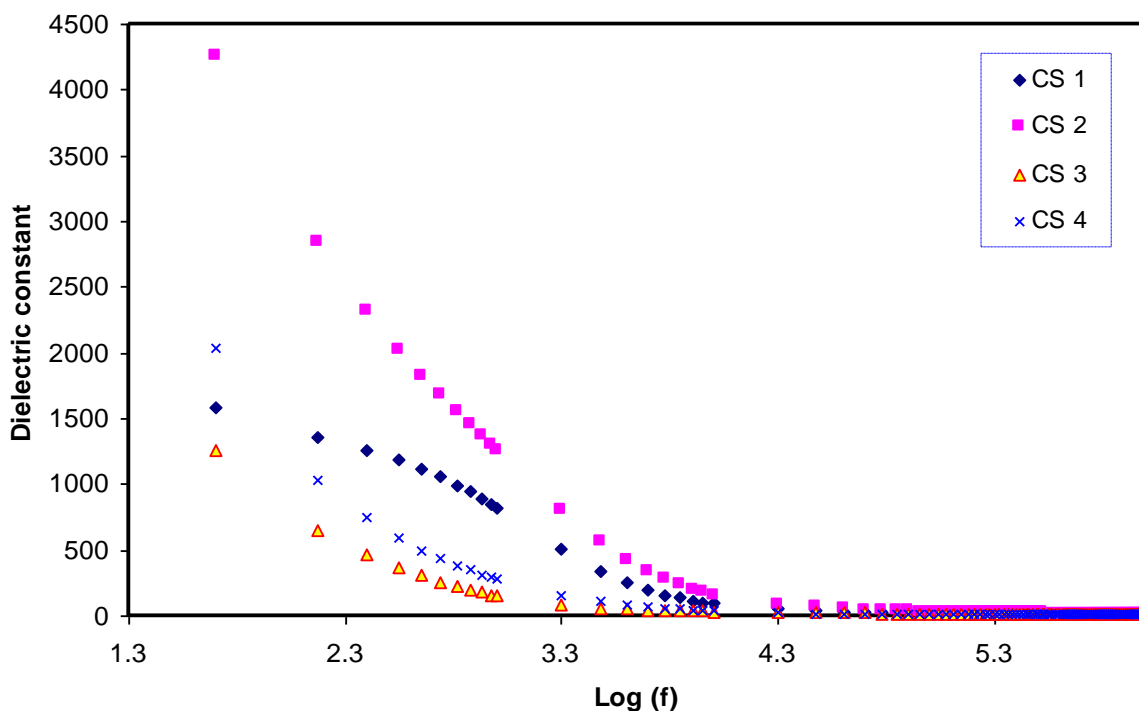

Figure 2. Variation of dielectric constant as a function of frequency for different CS:CuI solid polymer electrolytes at room temperature.
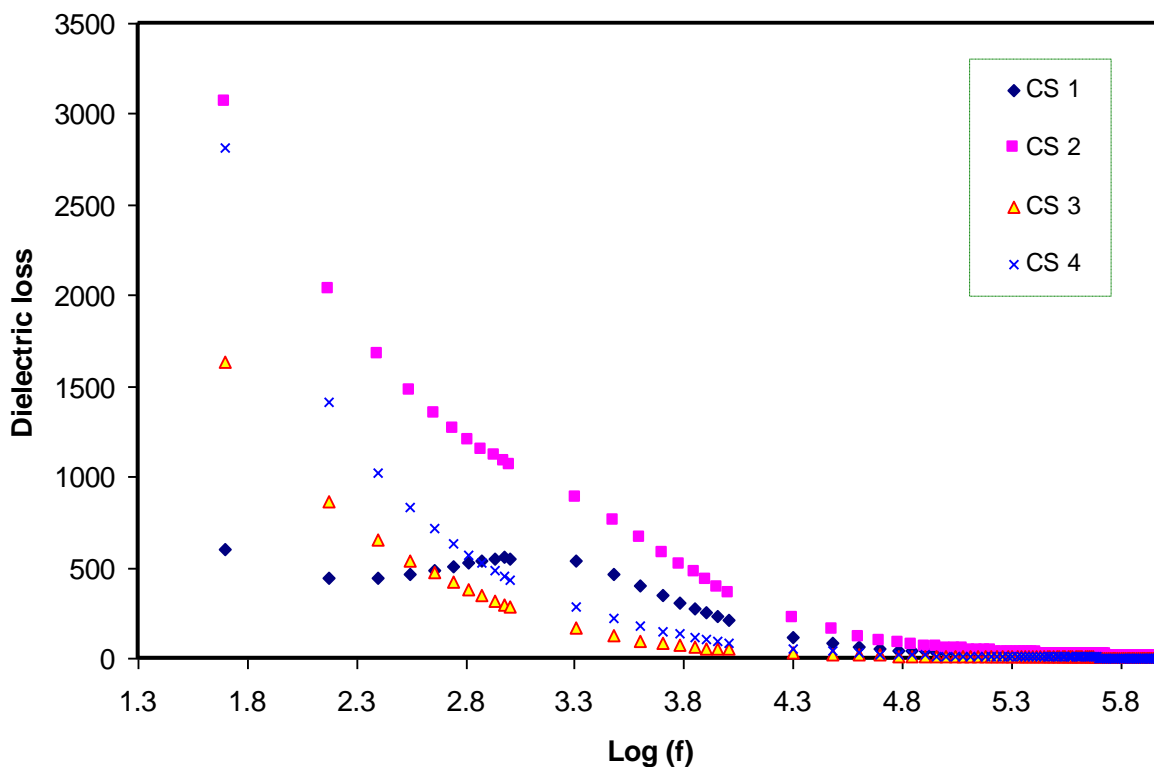
Figure 3. Variation of dielectric loss as a function of frequency for different CS:CuI solid polymer electrolytes at room temperature.

A typical result indicates that the CS incorporated with 8 wt.% CuI (CS2), has higher dielectric constant and dielectric loss at all frequency. However, any further increase in the CuI concentration caused the reduction of dielectric constant. The high value of dielectric constant for CS2 sample indicates that there is an increase in the number of charge carriers, and thus a high electrical conductivity. The frequency dependence of the ε_r and ε_i at higher salt concentration (> 8 wt.%) show very strong dispersions at low frequency due to space-charge polarization effects arising from accumulation of charge carriers at the electrode-electrolyte interface results in the formation of macro-dipoles that oscillate with the frequency of applied field, since there is time for the dipoles to build up at the interface before the occurrence of changes in the direction of applied field. These charge accumulations exhibit relaxation behavior similar to dipolar relaxation [31]. However, at high frequencies, the space-charge accumulation disappeared, and the dipoles cannot follow the high periodic reversal of the applied electrical field at the interface [32,33]. Thus, the contribution of the charge carriers towards polarization decreases, and hence, the values of ε_r decreases continuously with increasing frequency.

3.3 Ac conductivity analysis

The ac conductivity (σ_{ac}) of the polymer electrolyte films has been evaluated using the real (Z') and imaginary (Z'') parts of complex impedance (Z^*) data at a fixed temperature, using the following equation [34]:

$$\sigma_{ac} = \left[\frac{Z_r}{Z_r{}^2 + Z_i{}^2} \right] \left(\frac{l}{A} \right) \qquad (3)$$

The frequency dependent ac conductivity σ_{ac} at room temperature for all samples is shown in Fig. 4. The tail in ac conductivity (σ_{ac}) spectra at low-frequency region could be attributed to the accumulation of charge carriers at the electrode and polymer electrolyte interface [26]. In the high-frequency region, the value of σ_{ac} increase with increasing frequency and follows the power law ($\sigma_{ac} = A\omega^S$) [35]. It is well known that at high frequency the capacitive reactance ($X_c = 1/(2\pi f C)$), becomes small and thus the displacement current increases. Consequently, the AC conductivity increases. The extrapolation of the plateau region to the y-axis (zero frequency) was used to estimate the dc conductivity (σ_{dc}). The achieved dc ionic conductivities for all the polymer electrolytes are presented as the inset inside Figure 4. The σ_{dc} values achieved from the ac conductivity spectra are agree with the bulk resistance (R_b) shown in figure 1, that is, the system with low resistance exhibits a high DC conductivity.
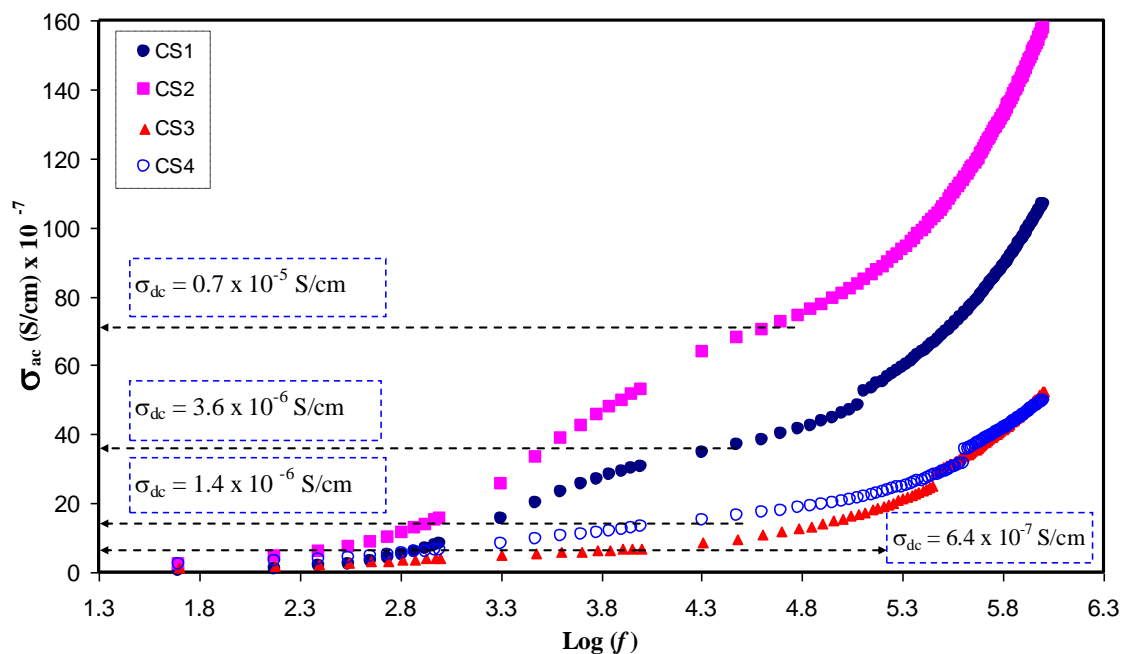

Figure 4. Variation of σ_{ac} as a function of frequency for all chitosan solid electrolytes system at room temperature. The CS2 sample exhibits a high DC conductivity.

Figure 5 shows the variation of ac conductivity σ_{ac} with frequency for CS3 sample at different temperatures. The conductivity spectrum for the sample with 12 wt.% salt concentrations (CS3) at low temperatures (303 and 323 K), consists of three regions: (i) a low-frequency dispersive region, (ii) an obvious plateau frequency region, and (iii) a high-frequency power-law region. The median frequency-region is due to the dc conductivity contribution while the high-frequency behavior represents a bulk relaxation phenomenon.

At higher temperatures (343 and 363 K), the frequency-dependent conductivity exhibits two distinct regions. It is clear that with an increase in temperature, the σ_{ac} frequency response shifts to the high-frequency dispersive region. A similar trend in frequency-dependent conductivity has been reported in the literature for different polymer electrolyte systems [36,37].
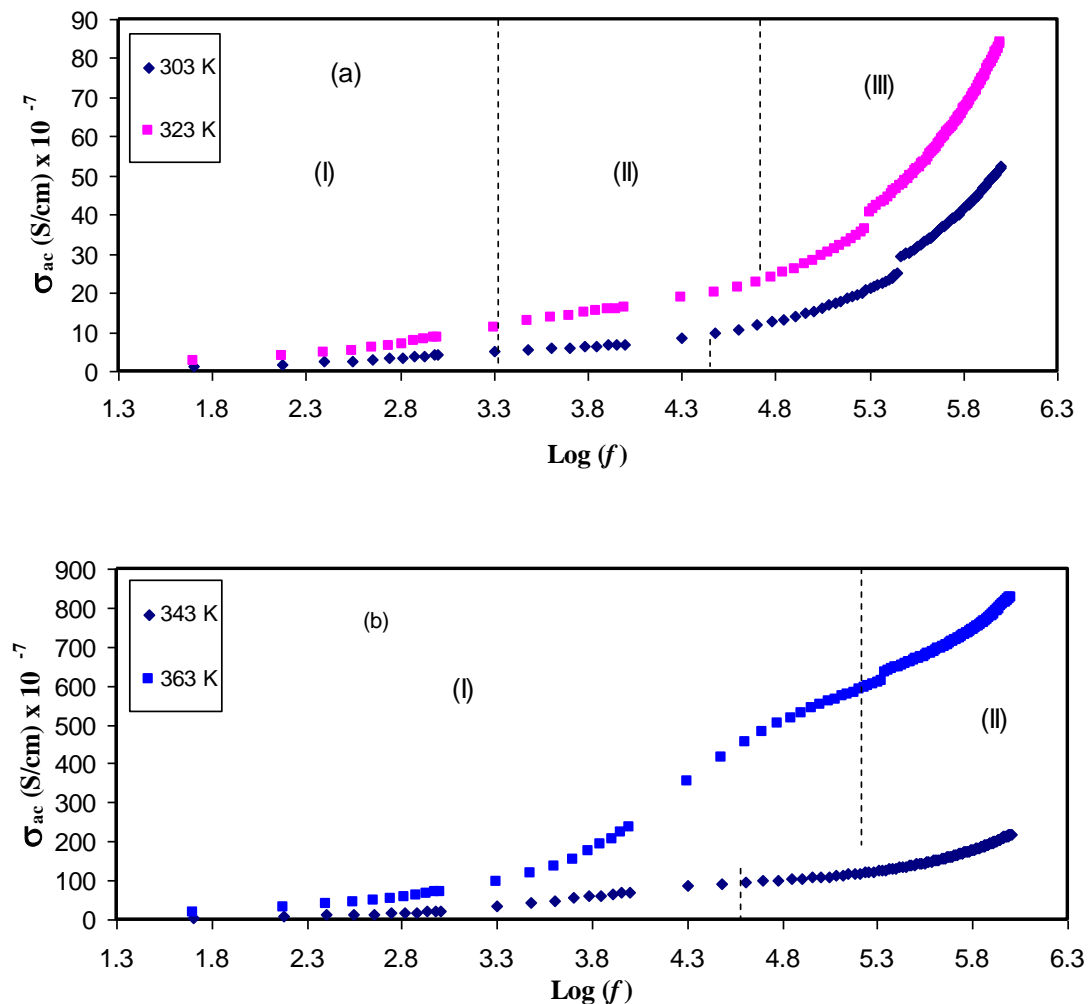

Figure 5. Variation of σ_{ac} as a function of frequency for CS3 sample at (a) 303 K and 323 K and (b) , 343 K and 363 K.

The frequency-dependent electrical conductivity behavior for the present polymer electrolyte system follows the Jonscher's universal power law [38].

$$\sigma(\omega) = \sigma_{dc} + A\omega^{S} \qquad (4)$$

where σ_{dc}, A, and S are the dc conductivity, pre-exponential factor, and frequency-exponent, respectively. At lower frequencies, ions are able to jump from one available site to another vacant neighboring site in the host polymer matrix and contribute to the dc conductivity. A successful hop occurs when the frequency is lower than the hopping frequency. The frequency-independent region at all temperatures signifies that the conductivity is equal to the bulk conductivity of solid polymer electrolytes [39]. At higher frequencies, the important feature $\sigma(\omega) \propto A\omega^S$ is observed. The ions perform correlated forward-backward hopping movement mechanism. These movements are potentially successful when ions jump and stay in the new site. Whereas the movements are unsuccessful hopping if the jumped ion jump back to its initial position [40]. The increase in the ratio of successful to unsuccessful hopping, results in a more dispersive conductivity at higher frequencies [41]. Such ionic motion occurs when the frequency exceeds the characteristic frequency corresponding to the onset of conductivity dispersion [13]. The values of S at different temperature were estimated for the power law regions, from the slope of $\log(\sigma)$ versus $\log(\omega)$. From the definition of frequency-exponent, the higher value of S reflects the poor conductivity of the sample.

The frequency exponent (S) as a function of temperature for the SC3 system were shown in figure 6. The continuous decrease in S value with increasing temperature reflects the increase in electrical conductivity of the sample. Several theoretical models have been proposed to explain the conduction mechanism based on the nature of the variation of S parameter with temperature. Among these models, the quantum mechanical tunneling (QMT), the small polaron (SP), the correlated barrier hopping (CBH) and the overlapping large polaron (OLP) are found to be the most applicable models [42]. The QMT model implies that S is temperature independent. The SP model indicates that conduction is predominant if S increases with increasing the temperature. The CBH model suggested that S should decrease with increasing temperature. Finally, the OLP model suggested that S should decrease with increasing temperature to a minimum value and then increases again [43]. In our system, the decreasing trend of S with temperature suggests that the CBH model is more convenient to interpret the conduction mechanism. It is important to notice that the CBH model consider the hopping of carriers between two sites over a potential barrier separating them [44]. The ac conductivity and frequency-exponent expressions due to the CBH model are given by the equation [42]:

$$S = 1 - \frac{6k_B T}{W_m - k_B T \ln(1/\omega\tau_o)} \qquad (5)$$

where W_m is the maximum barrier height that ions must overcome and τ_o is the characteristic relaxation time of the carriers.

For a small value of $k_B T \ln(1/\omega\tau_o) \ll W_m$ the equation (5) reduces to:

$$S = 1 - \frac{6k_B T}{W_m} \qquad (6)$$

The values of W_m can be calculated by putting values of S and T in equation (6). The characteristic increase in slope with the rise in temperature (slope of region II >> slope of region I) was due to the decrease in the binding energy.
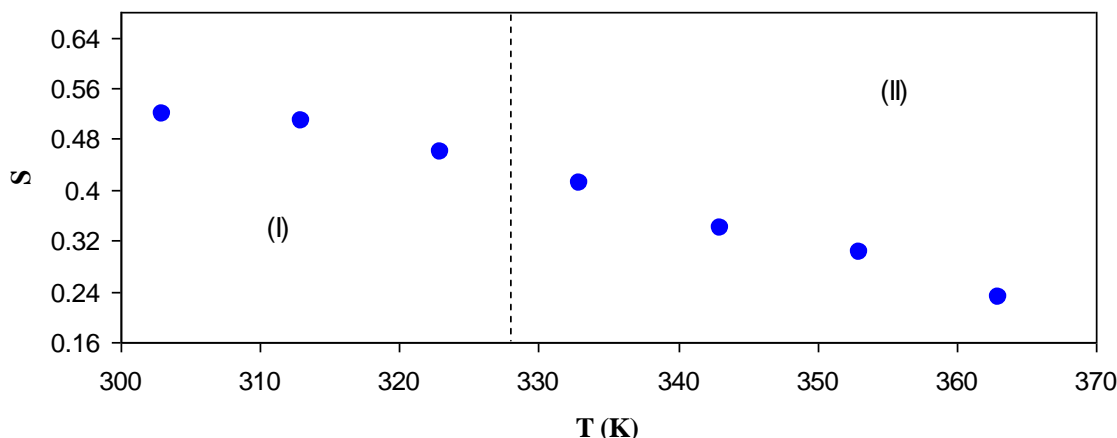

Figure 6. Temperature dependence of the frequency-exponent (s) for CS3.

3.4 Ionic conductivity analysis

The ionic conductivity of the polymer electrolyte films has been calculated from the bulk resistance (R_b) of the samples at various temperatures using the formula [45]:

$$\sigma_{dc} = l/R_b A \qquad (7)$$

The observed increase in ionic conductivity of CS:CuI polymer electrolyte films with temperature, obeys the Arrhenius type thermally activated process represented by:

$$\sigma_{dc} = \sigma_o \exp\left(\frac{-E_a}{k_B T}\right) \qquad (8)$$

where σ_o is the pre-exponential factor, E_a is the activation energy, k_B is the Boltzmann constant and T is the absolute temperature. Increase in temperature results in the increase in free volume, which lead to increases in ions mobility and segmental movement. The segmental dynamic of the polymer chains will either help the ions to hop from one site to another site or provide an alternative path for ions to move and thus increase the conductivity [46]. This hopping mechanism indicates that most of ions gained kinetic energy via thermally activated process [47]. Figure 7 shows the variation of dc conductivity versus reciprocal of temperature for CS3 sample. Clearly, two distinct regions can be seen. At low temperatures, the conductivity increases slowly. The possible explanation for low DC conductivity at low temperature is that ion transport occurs through the QMT process. It is clear from figure 6 that at low temperature the S value is almost temperature independent. These

results reveal that AC conductivity study is crucial for understanding the behavior of DC conductivity versus 1000/T. At high temperatures, an abrupt rise in DC conductivity can be observed in figure 7. At these temperatures, the S value (see figure 6) decreases to a minimum value. Thus at high temperatures, ion transport mechanism takes place through the hopping from one site to another and requires smaller activation energy [48]. The results of the present work, reveals that AC conductivity study can be combined with DC conductivity analysis to understand the ion transport mechanism. Thus to get deep insight about the conduction mechanism the frequency exponent (S) at different temperature must be studied.
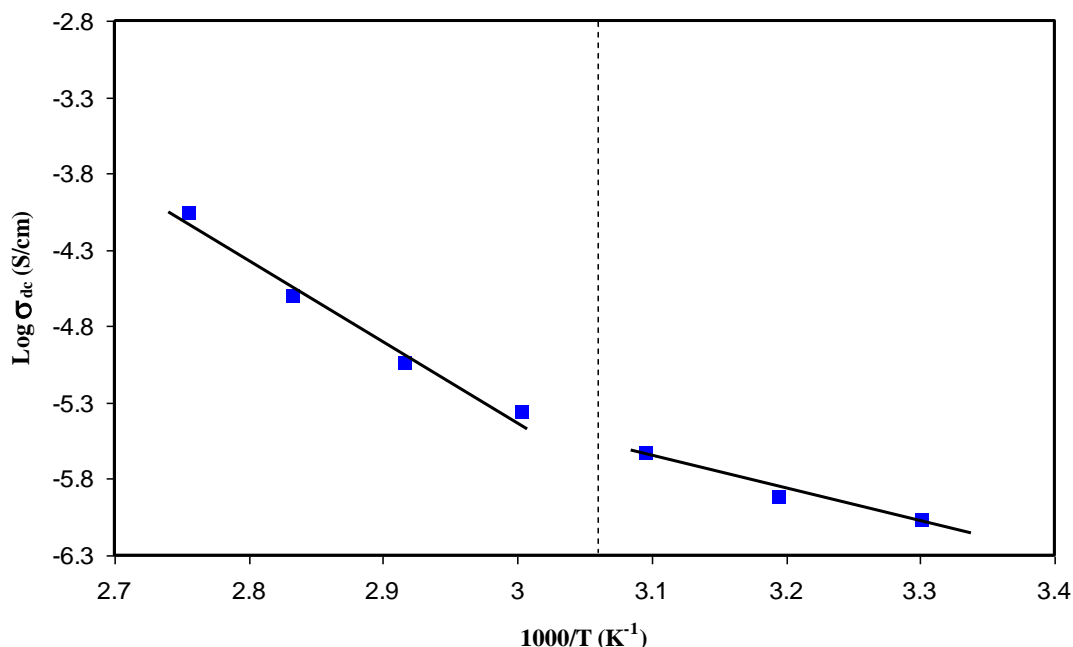

Figure 7. Inverse temperature dependent dc conductivity of CS+12 wt.% CuIpolymer electrolyte film (CS3).

3.5 Electric Modulus analysis

The electric modulus representation is convenient for the analysis of relaxation behavior of ionic materials. In electric modulus representation, the contributions of electrode polarization may be ignored [49]. The real (M') and imaginary (M'') parts of the complex electric modulus (M^*) were calculated from the real (Z_r) and imaginary (Z_i) parts of the complex impedance (Z^*) by using the following expression [37]:

$$M^* = M' + jM'' = j\omega C_o Z^* = \omega C_o Z_i + j\omega C_o Z_r \qquad (9)$$

Figure 8 shows the frequency dependence of M' spectra for different CuI salt concentration at room temperature. It is obvious from Fig.8, that M' values at lower frequencies are very small, and

tend to be zero which indicates the removal of electrode polarization contribution [46]. The increase of M' with increasing frequency may be due to the bulk effect.
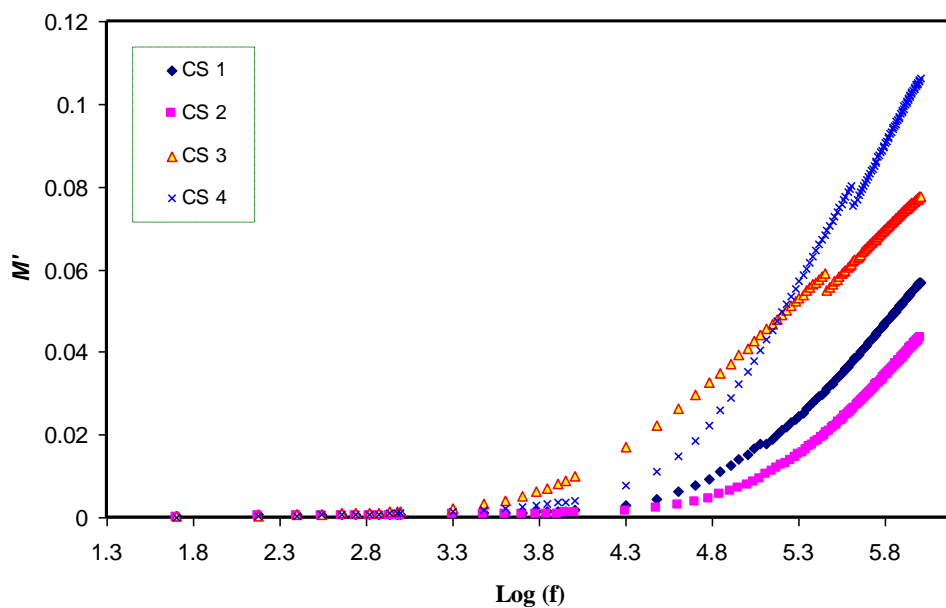

Figure 8. Variation of M' as a function of frequency for all the polymer electrolyte samples
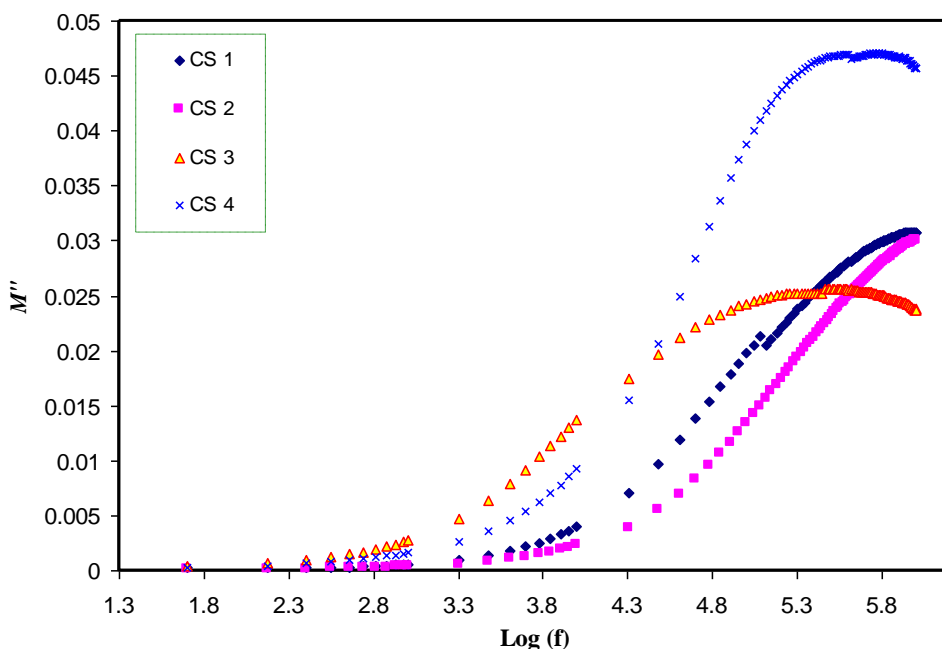

Figure 9. Variation of M'' as a function of frequency for all the polymer electrolyte samples

Figure 9 shows the variation of M'' with frequency for all CS:CuI solid polymer electrolyte films at room temperature. The observed long tail of M'' at low frequencies might be due to the large capacitance associated with the electrode polarization effect, results from the large charge carrier's accumulation at the electrode-solid polymer electrolyte interface [50]. The shifting of maximum peak

towards the higher frequency side at 8 wt.% CuI reveals that CS2 system is the highest conducting sample. The highest DC conductivity also achieved for the CS2 sample (see the insets of figure 4). Thus dielectric relaxation study is a good method to identify the conductivity behaviour of polymer electrolytes.

As shown in Fig. 9, the values of M'' show a broad and asymmetric peak in the high-frequency region, approximately centered in the dispersion region of M', predicts the non-Debye behavior.

The complex modulus spectrum (M'' versus M') for CS:CuI polymer electrolyte films at room temperature are shown in Fig. 10. According to Mohomed et al. [51], the emergence of single semicircular arc in Argand plots (M'' versus M') is an indicator for the ionic conductivity relaxation. But since the centre of the semicircular arcs are well localized below the real axis. Thus, the non-Debye type of relaxation is dominant and is evidence for the spread of the distribution of relaxation times [52]. The non existence of semicircular arcs with single relaxation time reveals that ion transport associated with the segmental motion of polymer chains. Consequently, copper ion transport through CS polymer occurs through the viscoelastic relaxation processes [40]. It can be seen that the samples with higher DC conductivity, their curves shifts more towards the origin. This is related to the low resistivity of these samples ($M'' = \omega C_o Z_r$) [12, 37].
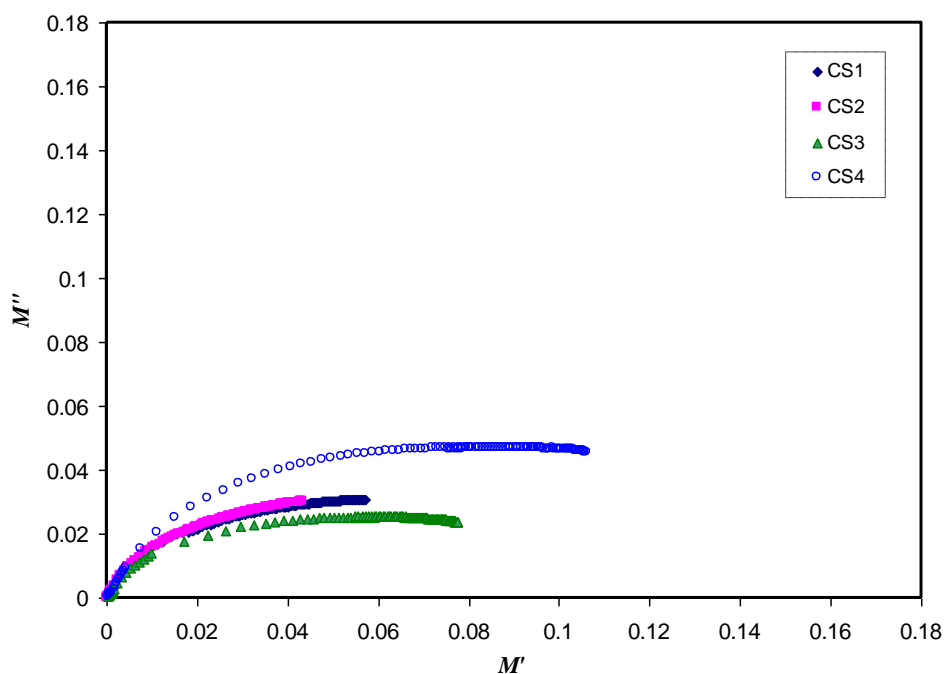

Figure 10. Complex modulus spectrum (M' vs. M'') for different CS:CuI polymer electrolyte films

4. CONCLUSIONS

Different composites of CS:CuI polymer electrolyte films have been prepared by solution cast technique. The dielectric analysis of the prepared films has confirmed the presence of electrode

polarization effects due to the accumulation of space charge polarization at lower frequencies. The ac conductivity spectra of polymer electrolytes obey Jonscher power law at higher frequency region. It has been observed that an increase of salt concentration increases ionic conductivity. Three regions were distinguished in the AC conductivity spectra of the present polymer electrolyte systems. The estimated DC conductivity from the extrapolation of the plateau region of frequency dependence AC conductivity was close to those values calculated using the bulk resistance obtained from the impedance plots. The dispersion regions of ac conductivity were used to study the copper ion conduction mechanism. Analysis of frequency exponent (S) at various temperatures suggested the correlated barrier hopping (CBH) model for ion transport mechanism at high temperatures, while at low temperatures the QMT model is more desired to interpret the behavior of DC conductivity versus 1000/T. The results of the present work, reveals that to get deep insight about the conduction mechanism the frequency exponent (S) at different temperature must be studied. To distinguish between ion conductivity relaxation and viscoelastic relaxation Argand plots was studied. The incomplete semicircular arcs with diameters below the real axis in Argand plots reveal that ion transport occurs with the help of segmental motion of polymer chains.

References

1. M.N. Chai, and M.I.N. Isa, *Sci. Reports*, 6 (2016) 27328.
2. S. B. Aziz, Z. H. Z. Abidin, and M. F. Z. Kadir, *Phys. Scr.*, 90 (2015) 035808 (9pp).
3. M.M.P. Madrigal, M.G. Edo, and C. Aleman, *Green Chem.*, 18(2016) 5930.
4. N.I. Harun, R.M. Ali, A.M.M. Ali, and M.Z.A. Yahya, *Ionics*, 18 (2012) 599.
5. A.S. Samsudin, W.M. Khairul, and M.I.N. Isa, *J. Non-Cryst. Solids*, 358 (2012) 1104.
6. M.F. Shukur, R. Ithnin, and M.F.Z. Kadir, *Ionics*, 20 (2014) 977.
7. Y. Yang, H. Hu, C.H. Zhou, S. Xu, B. Sebo, and X.Z. Zhao, *J. Power Sources*, 196 (2011) 2410.
8. S.R. Majid, and A.K. Arof, *Physica B: Condensed Matter*, 355 (2005) 78.
9. O.G. Abdullah, S.B. Aziz, and M.A. Rasheed, *Ionics* (2017). DOI:10.1007/s11581-017-2228-1
10. S.B. Aziz, O.G. Abdullah, and M.A. Rasheed, *J. Mater. Sci.: Mater. Electron.*, 28 (2017) 12873.
11. O.G. Abdullah, Y.A.K. Salman, and S.A. Saleem, *J. Mater. Sci.: Mater. Electron.*, 27 (2016) 3591.
12. S.B. Aziz, *Adv. Mater. Sci. Eng.*, 2016 (2016) 2527013 (11pp)
13. N. Shukla, A.K. Thakur, A. Shukla, and D.T. Marx, *Int. J. Electrochem. Sci.*, 9 (2014) 7644.
14. C.L. Lin, H.M. Kao, R.R. Wu, and P.L. Kuo, *Macromolecules* 35 (2002) 3083.
15. D. Golodnitsky, E. Strauss, E. Peled, and S. Greenbaum, *J. Electrochem. Soc.*, 162 (2015) A2551.
16. S. Mogurampelly, and V. Ganesan, *Macromolecules*, 48 (2015) 2773.
17. M.A. Webb, Y. Jung, D.M. Pesko, B.M. Savoie, U. Yamamoto, G.W. Coates, N.P. Balsara, Z.G. Wang, and T.F. Miller, *ACS Cent. Sci.*, 1 (2015) 198.
18. O.G. Abdullah, R.R. Hanna, and Y.A.K. Salman, *J. Mater. Sci.: Mater. Electron.*, 28 (2017) 10283.
19. S.B. Aziz, M.F.Z. Kadir, and Z.H.Z. Abidin, *Int. J. Electrochem. Sci.*, 11 (2016) 9228.

20. S.B. Aziz, R.M. Abdullah, M.A. Rasheed, and H.M. Ahmed, *Polymers*, 9 (2017) 338.
21. S.B. Aziz, Z.H.Z. Abidin, and A.K. Arof, *eXPRESS Polym. Lett.*, 4 (2010) 300.
22. S. Selvasekarapandian, R. Baskaran, and M. Hema, *Physica B: Condensed Matter*, 357 (2005) 412.
23. S.B. Aziz, *Bull. Mater. Sci.*, 38 (2015) 1597.
24. S.B. Aziz, Z.H.Z. Abidin, and A.K. Arof, *Physica B: Condensed Matter*, 405 (2010) 4429.
25. O.G. Abdullah, and S.A. Saleem, *J. Electron. Mater.*, 45 (2016) 5910.
26. S.B. Aziz, *Iran. Polym. J.*, 22 (2013) 877.
27. S. B. Aziz, *Nanomaterials*, 7 (2017) 444. doi:10.3390/nano7120444
28. N.H. Ahmad, and M.I.N. Isa, *J. Eng. Sci. Tech.*, 11 (2016) 839.
29. H.J. Woo, S.R. Majid, and A.K. Arof, *Mater. Chem. Phys.*, 134 (2012) 755.
30. M. Ravi, Y. Pavani, K.K. Kumar, S. Bhavani, A.K. Sharma, and V.V.R.N. Rao, *Mater. Chem. Phys.*, 130 (2011) 442.
31. M. Mudarra, R.D. Calleja, J. Belana, J.C. Canadas, J.A. Diego, J. Sellares, and M.J. Sanchis, *Polymer*, 42 (2001) 1647.
32. S. Ibrahim, S.M.M. Yasin, N.M. Nee, R. Ahmad, and M.R. Johan, *Solid State Commun.*, 152 (2012) 426.
33. S.B. Aziz, and Z.H.Z. Abidin, *Mater. Chem. Phys.*, 144 (2014) 280.
34. S.B. Aziz, O.G. Abdullah, M.A. Rasheed, and H.M. Ahmed, *Polymers*, 9 (2017) 187.
35. O. Gurbuz, B.F. Senkal, and O. Icelli, *Polym. Bull.*, 74 (2017) 2625.
36. S. B. Aziz, *Appl. Phys. A*, 122 (2016) 706.
37. S.B. Aziz, and Z.H.Z. Abidin, *J. Appl. Polym. Sci.*, 132 (2015) 41774.
38. A. K. Jonscher, *Nature*, 267 (1977) 673.
39. S. Ramesh, and C.W. Liew, *J. Non-Cryst. Solids*, 358 (2012) 931.
40. S.B. Aziz, M.A. Rasheed, and Z.H.Z. Abidin, *J. Electron. Mater.*, 46 (2017) 6119.
41. K. Funke, *Prog. Solid State Chem.*, 22 (1993) 111.
42. Z. Imran, M.A. Rafiq, M. Ahmad, K. Rasool, S.S. Batool, and M.M. Hasan, *AIP Advances*, 3 (2013) 032146.
43. S.M. Attia, M.S. Abdelfatah, and M.M. Mossad, *IOP Conf. Series: Journal of Physics: Conf. Series*, 869 (2017) 012035
44. A. Kahouli, A. Sylvestre, F. Jomni, B. Yangui, and J. Legrand, *J. Phys. Chem. A*, 116 (2012) 1051.
45. M.L. Verma, M. Minakshi, and N.K. Singh, *Ind. Eng. Chem. Res.*, 53 (2014) 14993.
46. S. Ramesh, and O.P. Ling, *Polym. Chem.*, 1 (2010) 702.
47. M. Premalatha, T. Mathavan, S.Selvasekarapandian, S. Selvalakshmi, and S.Monisha, *Org. Electron.*, 50 (2017) 418.
48. S.B. Aziz, M.A. Rasheed, S.R. Saeed, and O.G. Abdullah, *Int. J. Electrochem. Sci.*, 12 (2017) 3263.
49. L.N. Patro, and K. Hariharan, *Mater. Sci. Eng.*, B 162 (2009) 173.
50. A.S. Bhatt, D.K. Bhat, M.S. Santosh, and C. Tai, *J. Mater. Chem.*, 21 (2011) 13490.
51. K. Mohomed, T.G. Gerasimov, F. Moussy, and J.P. Harmon, *Polymer*, 46 (2005) 3847.
52. R. Ranjan, R. Kumar, N. Kumar, B. Behera, and R.N.P. Choudhary, *J. Alloy. Compd.*, 509 (2011) 6388.